# OFDM-PWM Scheme for Visible Light Communications

**Tian zhang[1], Zabih Ghassemlooy[2, *], Sujan Rajbhandari[3], Wasiu O. Popoola[4] and Shuxu Guo[1]**

*1. State Key Laboratory on Integrated Optoelectronics, College of Electronic Science and Engineering, Jilin University, Changchun, 130012, China;*
*2. Optical Communications Research Group, Faculty of Engineering and Environment, Northumbria University, Newcastle upon Tyne, NE1 8ST, U.K.*
*3. School of Computing, Electronics and Mathematics, Coventry University, Coventry, UK*
*4. Institute for Digital Communications, School of Engineering, the University of Edinburgh, UK*

**Abstract**: In this paper, we propose an improved hybrid optical orthogonal frequency division multiplexing (O-OFDM) and pulse-width modulation (PWM) scheme for visible light communications. In this scheme, a bipolar O-OFDM signal is converted into a PWM format where the leading and trailing edges convey the frame synchronization and modulated information, respectively. The proposed scheme is insensitive to the non-linearity of the light emitting diode (LED) as LEDs are switched 'on' and 'off' between two points. Therefore, the tight requirement on the high peak-to-average-power-ratio (PAPR) in O-OFDM is no longer a major issue. The simulation and experimental results demonstrate that the proposed scheme offers an improved bit error rate performance compared to the traditional asymmetrically clipped O-OFDM (ACO-OFDM).

## 1. Introduction

The rapid development of solid state lighting technologies has made the visible light communications (VLC) a promising complementary scheme to the widely used radio frequency (RF) based wireless communications in certain indoor and possibly outdoor applications [1]. The main challenge of the VLC technology is the lack of sufficiently high modulation bandwidth, which is associated with the white light emitting diodes (LEDs) having a very low modulation bandwidth $B_{\mathrm{LED}}$ (i.e., $B_{\mathrm{LED}} < 5$ MHz), hence limiting the transmission capacity [2]. In order to address this issue and make a good use of the limited $B_{\mathrm{LED}}$ with the aim of increasing the transmission throughput, a number schemes including (i) blue filtering at the receiver (Rx) to remove the slow phosphor part of the spectrum, which increases $B_{\mathrm{LED}}$ to ~ 20 MHz but at the cost of high power loss; (ii) high spectrally efficient modulation schemes, such as a variant of optical orthogonal frequency division multiplexing (O-OFDM), discrete multitone modulation (DMT) and multi-band carrier-less amplitude and phase modulation, have been extensively investigated in the literature [3-4]. In intensity modulation and direct detection (IM/DD) based VLC systems, the traditional complex and bipolar OFDM is modified to a real and unipolar format [5-8]. Though OFDM offers a number of advantages such as efficient use of the spectrum, there are a number of issues in OFDM based VLC systems including (a) a high peak-to-average-power-ratio (PAPR); (b) performance degradation due to non-linear power-current (P-I) characteristics of LEDs; (c) limited support for dimming; and (d) reduced throughput due to the use of longer cyclic prefix as a result of longer tails of the impulse response [9]. Among these, PAPR is by far the most detrimental to the performance of OFDM-VLC system. A higher PAPR leads to severe distortion and clipping because of the non-linear P-I characteristics of the LED [11]. This leads to a decreased signal-to-quantization noise ratio (SQNR) in both analog-to-digital (A/D) and digital-to-analog (D/A) converters while not fully utilizing the wide dynamic range of LEDs [12].

Considering that the indoor environment (i.e., the channel) is relatively static with no deep fading, the multipath induced interference is not a major issue as is the case in an outdoor

*Corresponding author.
*E-mail address:* z.ghassemlooy@northumbria.ac.uk

environment for RF-based wireless systems. Therefore, the use of OFDM in such environments would be mainly to increase the transmission data rate but at the cost of high PAPR. To address the high PAPR issue, a number of techniques have been proposed. Most of the work focus on reducing the PAPR using a pilot symbol (PS) [13] or linearizing the LED response [14]. However, there is still an open question: are there any advantages in transmitting the OFDM signal over a VLC channel or does it need to be converted into a digital format to avoid all the issues outlined above. To address this question, in this paper we propose an improved scheme for converting the OFDM signal into a pulse width modulation (PWM) format prior to IM of the LED in order to mitigate the requirement for higher PAPR values. A similar technique was proposed in [14] where a linear mapping function was used to covert OFDM samples into PWM, which was based on simulation. However, the required bandwidth of proposed scheme in [14] exceeds the O-OFDM scheme, thus leading to a bit error rate (BER) penalty. In our improved OFDM-PWM scheme, we take advantage of the anti-symmetry property of time-domain ACO-OFDM signal and hence covert only the first half samples of the ACO-OFDM frame and extend the pulse width of PWM by a factor $N_c$. This ensures the proposed OFDM-PWM has the same bandwidth requirement as of ACO-OFDM and the simulation and experimental results demonstrated an improved BER performance compared with the original ACO-OFDM. Furthermore, the advantages of the scheme in [14] such as resilience to LED non-linearity, reduced PAPR, higher luminance level are maintained.

The rest of the paper is organized as follows: the proposed OFDM-PWM VLC system is described in Section II followed by simulation results in Section III. Section IV presents the experimental proof-of-the-concept implementation with results. Finally, the concluding remarks are presented in Section V.

## 2. OFDM-PWM based VLC system description

The block diagram of proposed OFDM-PWM scheme is shown in Fig. 1, where the bipolar discrete-time O-OFDM samples $x(n)$ are first generated using the standard ACO-OFDM process as outlined in [15] but with no zero clipping operation prior to conversion to PWM. In the traditional O-OFDM such as DC-biased optical OFDM (DCO-OFDM), a DC bias is added to the signal before clipping the negative residual signals to ensure positive signal amplitude. However, due to a high PAPR, the DC bias required is very high and it is also necessary to clip the DC-biased signal to clip the negative residue. ACO-OFDM overcomes the high DC-biased requirements by encoding information only on odd harmonics and clipping the negative signals at zero, which does not lead to any information loss [15]. Due to the Hermitian symmetry requirements to ensure a real-time domain signal and with only odd subcarriers being used, only the $1/4^{th}$ of sub-carrier actually is encoded with the data. As a result, the spectral efficiency of ACO- OFDM is half that of DCO-OFDM [14].

Thus the resulting time domain signal is a real-valued signal referred to as the O-OFDM frame with the anti-symmetry property as defined by [16] and shown in Fig.1 (b):

$$x_k = -x_{k+N/2}, 0 < k < N/2 \ , \tag{1}$$

where $N$ is the number of IFFT points.

*Corresponding author.
*E-mail address:* z.ghassemlooy@northumbria.ac.uk

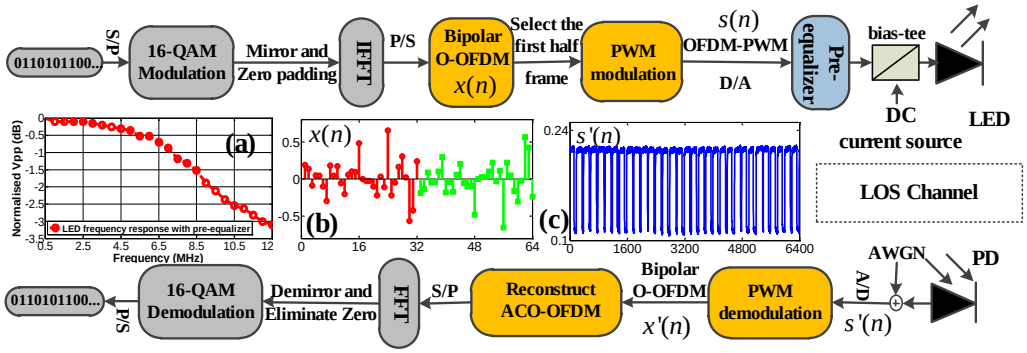


Fig. 1. Block diagram of OFDM-PWM (a) LED frequency response with pre-equalizer, (b) bipolar O-OFDM before asymmetrical clipping, (c) received OFDM-PWM waveform. S/P: serial-to-parallel converter, P/S: parallel-to-serial converter, PD: photodetector, LOS: line of sight.

In the OFDM-PWM scheme, since PWM can be used to linearly represent the bipolar signal, the zero clipping operation in ACO-OFDM is no longer necessary. Due to ACO-OFDM's anti-asymmetric time-domain characteristics, the first half bipolar samples (with no zero-clipping) are sufficient to represent the entire unipolar ACO-OFDM. Hence, instead of converting the entire O-OFDM symbol into PWM, converting only the first $N/2$ samples would be sufficient, which does not lead to any loss of information. Thus, we discard the unnecessary last half samples and save the half time slots for further compensating the high bandwidth requirement for PWM, see Fig. 2 (b) (blue line). The generated OFDM-PWM signal is used for IM of the LED. At the Rx the OFDM signal is extracted from OFDM-PWM and the standard OFDM demodulation process is thereafter employed, which is the reverse of the transmitter (Tx) process, as outlined in [16].

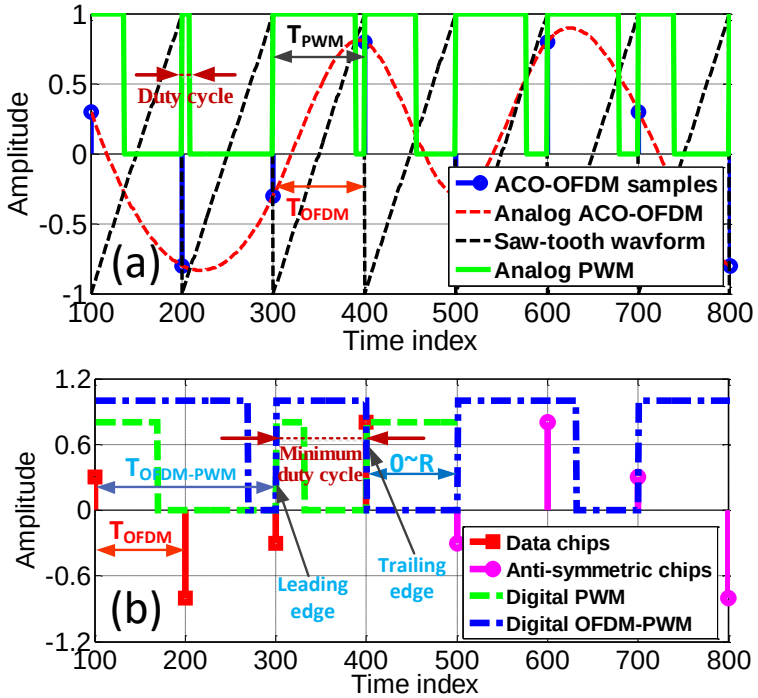


Fig. 2. Time domain waveforms for: (a) ACO-OFDM, ramp, and PWM, and (b) the process of the digital OFDM-PWM generation

PWM can be generated in the analogue or digital domain. In analogue PWM, the input signal (i.e., $x(n)$ in this case) is compared with a reference carrier signal (i.e., a ramp waveform) of frequency $f_c$ as shown in Fig. 2(a). Note that, in order to meet the Nyquist condition $f_c \geq 2NT_s^{-1}$, where $T_s$ is the OFDM symbol period. In digital PWM, the digital version of $x(n)$ is compared

*Corresponding author.
*E-mail address:* z.ghassemlooy@northumbria.ac.uk

with a counter, which rests every $2^L$, where $L$ is the bit resolution adopted in this paper. In the PWM scheme, the falling edge carries the information whereas the rising edge is used for synchronization (more information on PWM can be found in [17-19]). Thus, the converted PWM signal shown in Fig. 2(a) is given by:

$$PWM(t) = \begin{cases} C, & 0 \le t \le \tau \\ 0, & \tau < t \le T_c \end{cases}, \tag{2}$$

where $T_c$ is the OFDM symbol sampling period, $C$ is a constant corresponding to the peak amplitude of O-OFDM, and τ, given by (3), is the modulated pulse width that changes linearly with the instantaneous value of $x(n)$ as given by:

$$\tau(n) = \frac{x(n) - x_{\min}}{K}, \tag{3}$$

where $K$ is the PWM carrier signal slope factor or the modulation index defined as:

$$K = \frac{x_{\max} - x_{\min}}{T_c}. \tag{4}$$

Note that, $x_{max}$ and $x_{min}$ are the maximum and minimum amplitudes of O-OFDM symbols, respectively. In order to simplify generation of the digital PWM signal, the sampling period is divided into $R$-discrete intervals with $R \geq M$, where $M$ is QAM modulation order. Therefore, (3) and (4) are rewritten in a discrete form as:

$$K = \frac{x_{\max} - x_{\min}}{R} = \frac{(x(n) - x_{\min})}{N_\tau}, \ n = 1, \ldots, N/2, \tag{5}$$

where $N_\tau$ is the corresponding discrete intervals of $\tau(n)$.

In the converted PWM scheme, see Fig. 2(a), the minimum pulse duration $\tau(n)_{min} = 1/R$ is significantly smaller than $T_c$. Hence, the bandwidth requirement for PWM is $R$ times higher than ACO-OFDM. In order to overcome the high bandwidth requirement, the duty cycle of PWM signal is further extended by a factor of $N_c$, where $0 \le N_c \le R$ as shown in Fig. 2(b) with blue lines. The value of $N_c$ can be adjusted either to obtain a maximum throughput by setting $N_c = 0$ or a required dimming level by setting $N_c > 0$. In this study, we have increased the minimum pulse width to $R$ by setting $N_c = R$ (see Fig. 2(b)). This ensures that the PWM pulse duration is at least equal to or greater than $T_c$, which means the proposed OFDM-PWM scheme has the same bandwidth requirement as that of ACO-OFDM. In addition, due to the increased time factor $N_c$ is equal to the OFDM sample period, which means we take full advantage of the last half time slots saved from the previous sampling part. Thus, the transformation from ACO-OFDM to OFDM-PWM is a lossless process. The proposed OFDM-PWM signal $s(n)$ is given by:

$$s(n) = \begin{cases} C, 0 \le N_{s(n)} \le (N_\tau + N_c) \\ 0, (N_\tau + N_c) < N_{s(n)} \le 2R \end{cases}, n = 1, \ldots, N/2, \tag{6}$$

where $N_s(n)$ is the total number of discrete intervals corresponding to the duty cycle of each OFDM-PWM signal.

Following optical to electrical (O-E) conversion at the Rx, the received OFDM-PWM signal $s'(n)$ is given by:

*Corresponding author.
*E-mail address:* z.ghassemlooy@northumbria.ac.uk

$$s'(n) = \eta F\left[x(n)\right] \otimes h(n) + z(n) \ , \tag{7}$$

where $\eta$ is the photodiode responsivity, $F[\,.\,]$ is the transformation operation from O-OFDM to PWM, $x(n)$ is the bipolar O-OFDM signal, $h(n)$ is the channel impulse response, $z(n)$ is additive white Gaussian noise [20] with zero mean and variance of $\delta_z^2$, and $\otimes$ denotes the convolution operation. Note that, here we have only considered the line of sight propagation path in order to illustrate the concept.

As for recovery of the original OFDM signal at the Rx, the sampling rate of OFDM-PWM must be at least $2R$ times of the ACO-OFDM signal to accurately detect the trailing edge of $s'(n)$. The total number of discrete intervals of $s'(n)$ i.e., $(N_t+N_c)$ is then estimated from the trailing edge position, and the first half of $x(n)$ is estimated using (5). Next, the standard ACO-OFDM demodulation process outlined in [3] is adopted to recover the transmitted signal.

PAPR is a key factor in limiting the performance of O-OFDM systems [9]. The PAPR of discrete O-OFDM signal $x(n)$ is defined as the ratio of the maximum instantaneous power to the average power, which is given by:

$$PAPR = \frac{\max\left|x(n)\right|^2}{E\left[\left|x(n)\right|^2\right]}, \tag{8}$$

where E[.] denotes the statistical expectation. PAPR can be considered as a random variable, and is best characterized by the complementary cumulative distribution function (CCDF), which measures the effectiveness of PAPR reduction schemes, that denotes the probability that PAPR of an OFDM signal exceeds a certain threshold $\mathrm{PAPR}_0$ as given by [8]:

$$CCDF = P\left(PAPR > PAPR_0\right) = 1 - P(PAPR \le PAPR_0) = 1 - CDF \ . \tag{9}$$

In addition to a higher illumination level, the proposed OFDM-PWM offer reduced PAPR in comparison to ACO-OFDM, which can be advantageous in dynamic range limited systems. The simulation results for the average optical power and PAPR is presented in the following sections.

## 3. Simulation results

Since the average duty cycle of OFDM-PWM is greater than $T_c$, the proposed OFDM-PWM scheme provides a higher illumination level provided $C$ is equal to the maximum amplitude of ACO-OFDM sample as shown in Fig. 3.

*Corresponding author.
*E-mail address:* z.ghassemlooy@northumbria.ac.uk

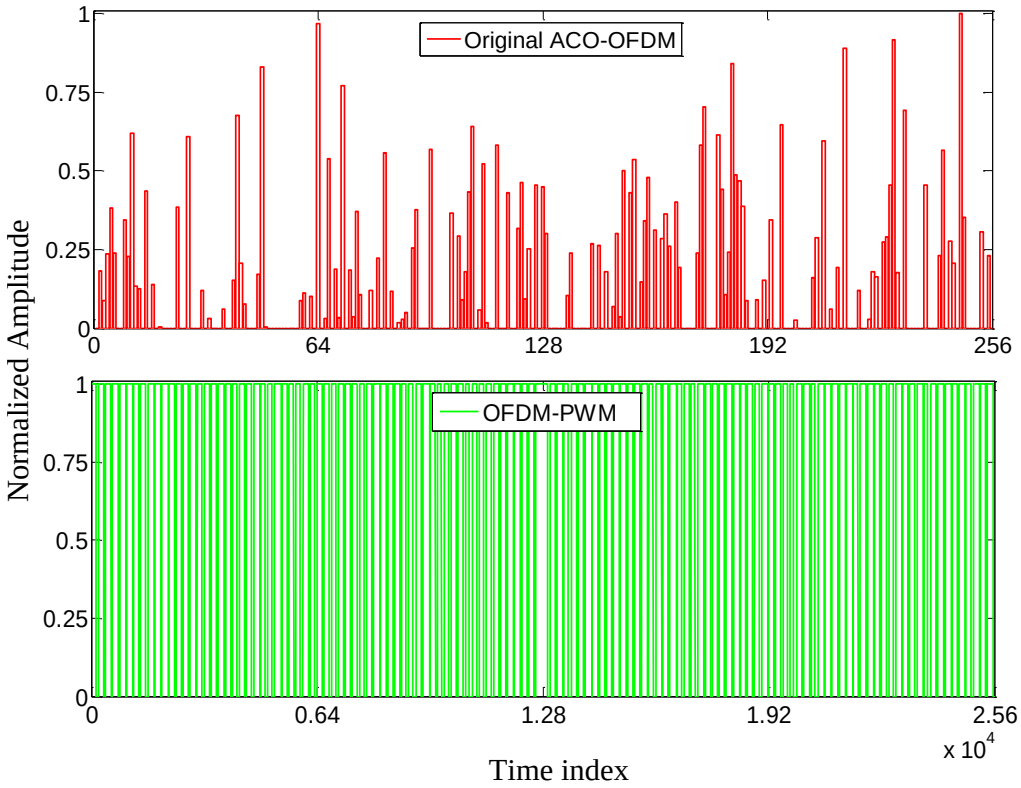


Fig. 3. One frame of ACO-OFDM and OFDM-PWM with the same data information (*R*=100 and 256 subcarriers)

Here, we calculate the average optical power of ACO-OFDM and OFDM-PWM to illustrate the illumination level. For the frame shown in Fig. 3, the average power of OFDM-PWM is ~4 times as much as the original ACO-OFDM frame. Therefore, *C* can be set to be smaller than the maximum amplitude of ACO-OFDM sample to achieve the desired illumination level and resilience to the $PAPR_0$ limit due to the non-linearity of the LED. Fig. 4 shows the simulated PAPR for ACO-OFDM, ACO-OFDM with classical selected mapping (SLM) technique [10] and the proposed OFDM-PWM method. Here, 16-QAM ACO-OFDM with 256-subcarrier is used as the PAPR reference. The SLM method with 6 iterations is employed to compare with proposed OFDM-PWM. Fig. 4 demonstrates that PAPR requirements at CCDF of $10^{-3}$ are ~3 dB, >12 dB and <16 dB for OFDM-PWM, ACO-OFDM with SLM and ACO-OFDM, respectively. This clearly validates that the proposed OFDM-PWM offers significant PAPR reduction.

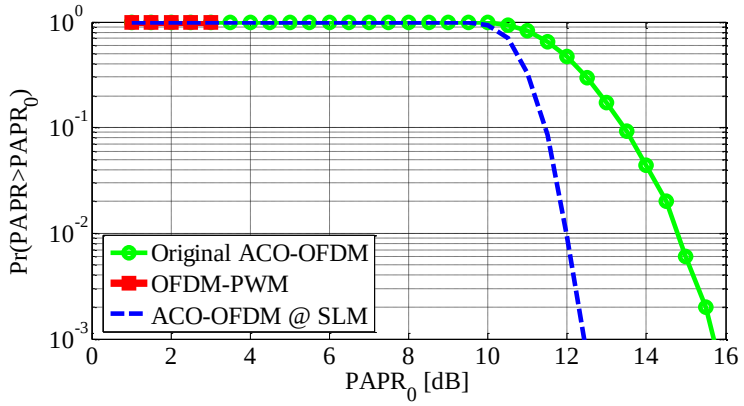


Fig. 4. PAPR analysis for 16-QAM ACO-OFDM signals (*N*=256), with SLM and OFDM-PWM.

*Corresponding author.
*E-mail address:* z.ghassemlooy@northumbria.ac.uk

Next, we have evaluated the BER performance of the proposed scheme for a line of sight (LOS) VLC link in Matlab environment. The key simulation parameters adopted in this work are summarized in Table I.

TABLE I
SIMULATION PARAMETERS

| Parameters | OFDM-PWM | ACO-OFDM |
|---|---|---|
| **Modulation** | 16/64-QAM | 16/64-QAM |
| **No of subcarriers** | 256 | 256 |
| **System bandwidth** | 10 MHz | 10 MHZ |
| **Date rate** | 40/60 Mbit/s | 40/60 Mbit/s |
| **Subdivisions** | *R*=100/256 | -- |
| **Length of frame** | 25600/65536 | 256 |
| **Iteration** | 1000 | 1000 |

Since the pulse width variation in PWM is linearly proportional to the peak-to-peak amplitude $v_{\text{p-p-OFDM}}$ of the input signal (i.e., in this case, the O-OFDM), then we need to know the time resolution corresponding to the amplitude resolution of the O-OFDM signal [21]. We have selected a nominal value of *R* as given by:

$$R = \begin{cases} 100, & M \le 16 \\ \alpha M, & M > 16 \end{cases}, \tag{10}$$

where α is an empirical constant, which is set to be 4 in our simulation, and *M* is the QAM modulation order. For example, the values of *R* for 16- and 64-QAM are 100 and 256, respectively

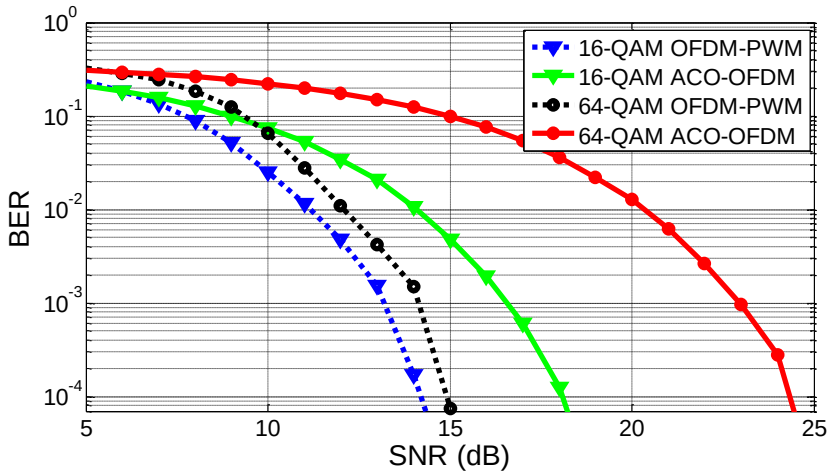


Fig. 5. The BER performance against the electrical SNR for OFDM-PWM and ACO-OFDM and with 16- and 64-QAM

Fig. 5 shows the simulated BER performance against the electrical SNR for OFDM-PWM and ACO-OFDM with 16- and 64-QAM. The simulation results clearly demonstrate that the OFDM-PWM outperform ACO-OFDM. For example, at a BER of $10^{-4}$ the SNR requirements are ~14 dB and ~18 dB for OFDM-PWM and ACO-OFDM, respectively for 16-QAM, thus demonstrating a SNR gain of ~4 dB using OFDM-PWM. The SNR gain is higher for the higher order modulation with 64-QAM OFDM-PWM offering a gain of ~9 dB compared to ACO-OFDM.

## 4. Experiment Results and Discussions

The experimental set-up shown in Fig. 6 has been developed to demonstrate the working

*Corresponding author.
*E-mail address:* z.ghassemlooy@northumbria.ac.uk

principle of the proposed concept, validate the simulation results and compare it with the standard ACO-OFDM under the same conditions. The frame frequency and frame sampling rate are shown in Table II.

TABLE II
EXPERIMENTAL PARAMETERS

| Parameters | OFDM-PWM | ACO-OFDM |
|---|---|---|
| **Frame frequency $f_{frame}$** | 39 kHz | 39 kHz |
| **Frame sampling $f_{sample}$** | 5 Gsample/s | 50 Msample/s |
| **DC-bias current** | 200 mA | 200 mA |
| **Modulation** | 16-QAM | 16-QAM |
| **No of random bits** | 256 | 256[1] |

[1] only 1/4 of the subcarrier are allocated for information bits in ACO-OFDM.

Firstly, we generated 16-QAM based ACO-OFDM and OFDM-PWM signals using the algorithm outlined in Section 2. The waveforms are then loaded to the arbitrary function generator (Tektronix AFG 3022) using the LabVIEW 2014 interface. Following this, the output signal was pre-equalized using a simple resistance-capacitance (RC) network, see Fig. 6(c), and a DC-bias current $I_{dc}$ of 200 mA was added prior to IM of the LED (Rebel Star 01). Note that, $I_{dc\text{-}ACO\text{-}OFDM} < I_{dc\text{-}DCO\text{-}OFDM}$, which is mainly used for illumination [22]. Use a RC pre-equalizer network $B_{LED}$ is increased from ~2 MHz to 12 MHz [23] as shown in Fig. 1(a).

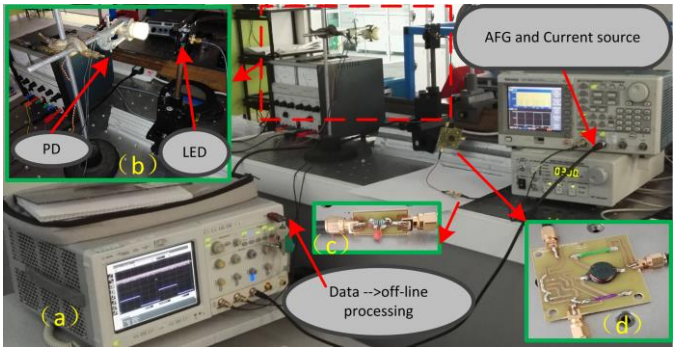


Fig. 6. (a) The experimental setup for the proposed Scheme. (b) the LED and PD, (c) the RC equalizer circuit, and (d) the DC-bias circuit

In practical VLC systems, LED non-linearity is important and should be considered, limits the operating dynamic range, $PAPR_0$ and consequently the SNR. Non-linearity arises due to the imperfection of the driving circuits and the number of emitted photons not directly being proportional to the injected current in the active region. The measured I-V curve for the LED used in this work is depicted in Fig. 7, which shows linear and non-linear region. A lower limit is as the turn-on voltage (TOV) and the saturation voltage.

*Corresponding author.
*E-mail address:* z.ghassemlooy@northumbria.ac.uk

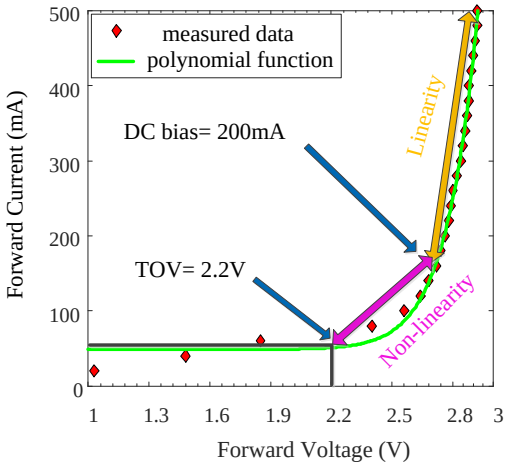


Fig. 7. The LED I-V plot using polynomial function (Rebel Star 01, LED). TOV: Turn-on voltage

The Rx front-end consists of an optical concentrator and a photodiode with differential amplifiers the outputs of which are captured using a digital oscilloscope (Agilent Infinium 40GSa/s) for further off-line processing. The oscilloscope sampling rates were set to 50 Msample/s and 5 Gsample/s for ACO-OFDM and OFDM-PWM, respectively. Signals synchronization, down-sampling, and signal recovery were carried out off-line. We then evaluated the BER performance of both ACO-OFDM and OFDM-PWM systems under the same conditions. For high order modulations (i.e., 64-QAM) the generated digital OFDM-PWM's length is 65536, which is beyond the 32K memory of AFG 3022. Therefore, we could only transmit one frame of 16-QAM based 256-subcarrier OFDM-PWM due to the limited memory of AFG3022. The received waveforms of ACO-OFDM and OFDM-PWM are shown in Figs. 8 (a) and (b), respectively. The square waveforms shown are used to indicate the period of the OFDM signals. Following off-line processing, the original ACO-OFDM signal is fully recovered as shown in Fig. 8 (c).

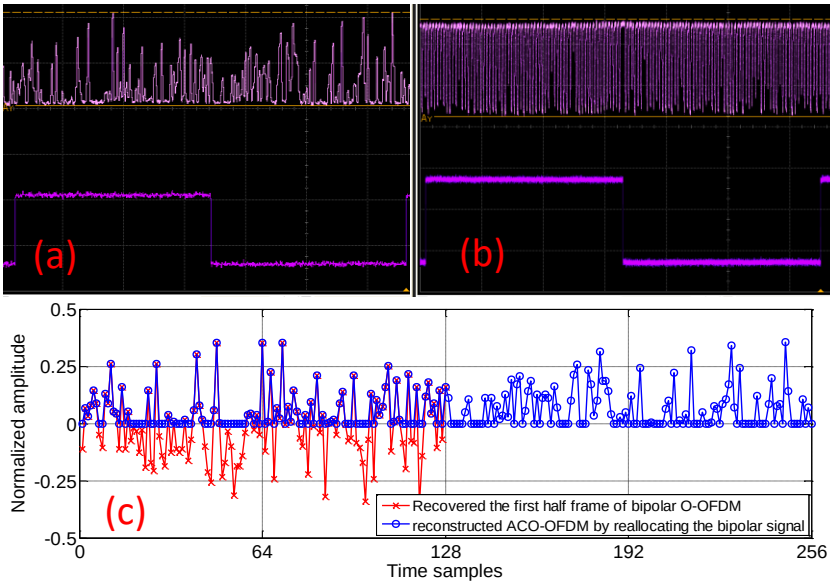


Fig. 8. Waveforms of: a single frame of 256-subcarrier for: (a) ACO-OFDM, (b) OFDM-PWM with *R*=100, and (c) the recovered half frame of bipolar signal and the reconstructed ACO-OFDM frame. Note, the square wave in (a) and (b) is to show the period of OFDM waveforms.

Fig. 9 shows the estimated BER performance, which is obtained experimentally, against the

*Corresponding author.
*E-mail address:* z.ghassemlooy@northumbria.ac.uk

peak-to-peak amplitude $V_{p-p}$ values of 16-QAM based ACO-OFDM and OFDM-PWM signals. Due to a limited number of transmitted bits, it was not feasible to accurately measure BER below the FEC limit of $10^{-3}$. Nonetheless, the graph clearly demonstrates the advantage of OFDM-PWM over ACO-OFDM, where it displays an improved BER performance in both linear and non-linear regions of the LED. For $V_{p-p} < 2$ V, the BER floor for OFDM-PWM is $< 5\times10^{-3}$, whereas for ACO-OFDM it is $> 10^{-1}$, except at $V_{p-p}$ of 2, where the BER is $10^{-2}$. For $V_{p-p} > 2$ V the BER performance shows degradation for both schemes. However, OFDM-PWM is still superior to ACO-OFDM. Since the information is carried in the pulse width, rather than pulse amplitude as in ACO-OFDM, OFDM-PWM displays a higher resilience to the non-linearity of the LED and clipping, thus offering an improved performance.

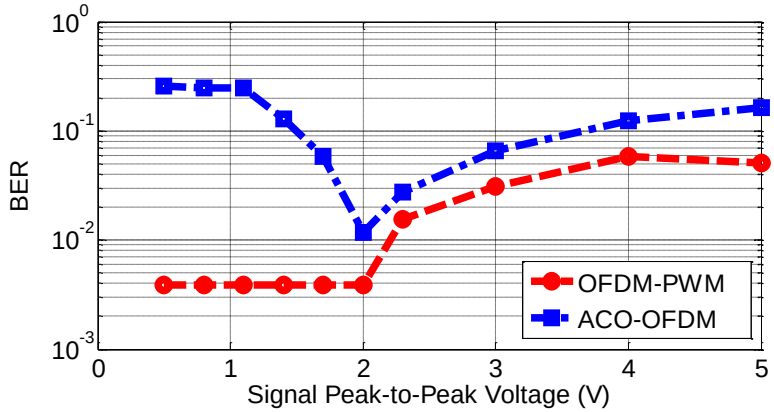


Fig. 9. Experimental BER against the peak to peak amplitude for 16-QAM OFDM-PWM and ACO-OFDM under the same conditions.

## 5. Conclusion

In this paper, an improved modulation scheme based on the conversion of an ACO-OFDM signal to PWM was proposed and studied. The OFDM-PWM offers significant advantages compared with the traditional ACO-OFDM scheme including lower PAPR, higher luminance, improved BER performance and enhanced resilience to the source non-linearity. The simulation and experimental results showed that a significant BER improvement can be achieved with OFDM-PWM compared with ACO-OFDM, thus demonstrating the potential of the proposed scheme. The future work includes optimization of the proposed scheme, analytical study of the BER performance and further experimental verifications.

## Acknowledgments

This research was supported by the University of Northumbria upon Tyne and Jilin University, and author T. Zhang is grateful to China Scholarship Council for the scholarship received (Grant. 201506170113).

## References

[1] Z. Ghassemlooy, S. Arnon, M. Uysal, X. Zhengyuan, and C. Julian, "Emerging Optical Wireless Communications-Advances and Challenges," *Sel. Areas Commun. IEEE J.*, 33(2015) 1738-1749.

[2] H. Le Minh, D. O'Brien, G. Faulkner, Z. Lubin, L. Kyungwoo, J. Daekwang, O. Yunje, and W. Eun Tae, "100-Mb/s NRZ visible light communications using a postequalized white LED," *IEEE Photonics Technol. Lett.*, 21(2009) 1063-1065.

[3] S. D. Dissanayake and J. Armstrong, "Comparison of ACO-OFDM, DCO-OFDM and ADO-OFDM in IM/DD systems," *J. Light. Technol.*, 31(2013) 1063-1072.

[4] K Werfli, P. A Haigh, Z. Ghassemlooy, "Multi-band carrier-less amplitude and phase modulation with decision feedback equalization for bandlimited VLC systems, " *Optical Wireless Communications (IWOW)*, 2015 4th *International Workshop on. IEEE*, pp: 6-10, 2015.

[5] H. Kimura, K. Asaka, H. Nakamura, S. Kimura, and N. Yoshimoto, "Energy efficient IM-DD OFDM-PON

*Corresponding author.
*E-mail address:* z.ghassemlooy@northumbria.ac.uk

using dynamic SNR management and adaptive modulation.," *Opt. Express*, 22(2014) 1789-1795.
[6] A. H. Azhar, T. Tran, and D. O. Brien, "A Gigabit / s Indoor Wireless Transmission Using MIMO-OFDM visible-light communications," *IEEE Photonics Technol. Lett.*, 25(2013) 171-174.
[7] Z. Ghassemlooy, W. O. Popoola, and S. Rajbhandari, "Optical Wireless Communications – System and Channel Modelling with Matlab", *CRC publisher*, New York, USA, 2012.
[8] J. Armstrong, "OFDM for optical communications," *J. Light. Technol.*, 27(2009) 189-204.
[9] T. Tao Jiang and Y. Yiyan Wu, "An Overview: Peak-to-Average Power Ratio Reduction Techniques for OFDM Signals," *IEEE Trans. Broadcast.*, 54(2008) 257-268.
[10] T. zhang, Z. Ghassemlooy, C.Y. Ma and S. X. Guo, "PAPR reduction scheme for ACO-OFDM based visible light communication systems," *Opt. Commun.*, 383(2017) 75-80.
[11] B. Inan, S. C. Jeffrey Lee, S. Randel, I. Neokosmidis, A. M. J. Koonen, and J. W. Walewski, "Impact of LED Nonlinearity on Discrete Multitone Modulation," *J. Opt. Commun. Netw.*, 1(2009) 439-451.
[12] R. Mesleh, H. Elgala, and H. Haas, "LED Nonlinearity Mitigation Techniques in Optical Wireless OFDM Communication Systems," *J. Opt. Commun. Netw.*, 4(2012) 865-875.
[13] W. O. Popoola, Z. Ghassemlooy, and B. G. Stewart, "Pilot-Assisted PAPR Reduction Technique for Optical OFDM Communication Systems," *J. Light. Technol.*, 32(2014) 1374-1382.
[14] V. Guerra, C. Suarez-Rodriguez, O. El-Asmar, et al, "Pulse width modulated optical OFDM," *International Conference on Communication Workshop (ICCW), IEEE*, pp.1333-1337, 2015.
[15] A. M. Khalid, G. Cossu, R. Corsini, et al, "1-Gb/s transmission over a phosphorescent white LED by using rate-adaptive discrete multitone modulation," *IEEE Photonics J.*, 4(2012) 1465-1473.
[16] J. Armstrong, B. J. C. Schmidt, "Comparison of asymmetrically clipped optical OFDM and DC-biased optical OFDM in AWGN," *IEEE Commun. Lett.*, 12(2008) 343-345.
[17] B. Wilson and Z. Ghassemlooy, "Pulse time modulation techniques for optical communications: a review," *IEE Proc. J Optoelectron.*, 140(1993) 347-357.
[18] P. D. Olcott, S. Member, and C. S. Levin, "Pulse Width Modulation : a Novel Readout Scheme for High Energy Photon Detection," *IEEE in Nuclear Science Symposium Conference Record*, NSS'08, pp. 4530-4535, Oct. 2008
[19] M. Barr, "Pulse width modulation," *Embedded Systems Programming*, 14(2001) 103-104.
[20] F. Li, K. Wu, W. Zou, and J. Chen, "Optimization of LED's SAHPs to simultaneously enhance SNR uniformity and support dimming control for visible light communication," *Opt. Commun.*, 341(2015) 218-227.
[21] C. R. Berger, Y. Benlachtar, and R. Killey, "Optimum Clipping for Optical OFDM with Limited Resolution DAC/ADC," *Sppcom*, no. 1, p. SPMB5, Jun.2011.
[22] X. Ling, S. Member, J. Wang, S. Member, and X. Liang, "Offset and Power Optimization for DCO-OFDM in Visible Light Communication Systems," 64(2016) 349-363.
[23] P. A. Haigh, Z. Ghassemlooy, H. Le-Minh, S. Rajbhandari, F. Arca, S. F. Tedde, O. Hayden, and I. Papakonstantinou, "Exploiting Equalization Techniques for Improving Data Rates in Organic Optoelectronic Devices for Visible Light Communications," *Light. Technol. J.*, 30(2012) 3081-3088.

*Corresponding author.
*E-mail address:* z.ghassemlooy@northumbria.ac.uk